Collisional Merging of Field-Reversed Configurations in the FAT-CM Device Form Targets for the Excitation of Low-Frequency Waves*)

Akiyoshi HOSOZAWA, Tomohiko ASAI, Tsutomu TAKAHASHI, Junichi SEKIGUCHI, Kouji HIROHASHI, Sigefumi OKADA, Hiroshi GOTA[1], Thomas ROCHE[1], Michiaki INOMOTO[2] and Toshiki TAKAHASHI[3]

College of Science and Technology, Nihon University, Tokyo 101-8308, Japan
[1] *TAE Technologies, Inc., CA 92610, USA*
[2] *Graduate School of Frontier Science, The University of Tokyo, Kashiwa 277-8561, Japan*
[3] *Graduate School of Engineering, Gunma University, Kiryu 376-8515, Japan*

(Received 30 September 2018 / Accepted 8 January 2019)

We have conducted collisional merging of field-reversed-configuration (FRC) plasmas in the FAT-CM (FRC Amplification *via* Translation–Collisional Merging) device to generate merged FRCs as targets for the excitation of low-frequency waves. Because of the high-beta nature of an FRC, the confining magnetic field is highest at the wall of the device and decreases toward a magnetic null inside the separatrix. We therefore find that the frequencies of the waves produced in this experiment must be lower than the ion cyclotron frequency or higher than the electron plasma frequency, because waves outside this band are reflected or resonant outside the separatrix of the FRC. We have therefore developed loop antennas and power supplies to apply low-frequency, oscillatory magnetic fields and have installed them in the FAT-CM device. The parameters characterizing the equilibrium phase of the merged FRC (lifetime ∼250 μs, radius ∼0.2 m, length ∼1.8 m, electron density ∼1.0 $\times 10^{20}$ m^{-3}, and total temperature ∼100 eV) are sufficient to enable studies of the propagation of low-frequency waves in the core regions of FAT-CM FRCs. We have also performed an initial experiment in which an oscillatory magnetic field has been applied to a merged FRC.

Keywords: compact toroid, field-reversed configuration, low-frequency wave heating

DOI: 10.1585/pfr.14.2402041

1. Introduction

A field-reversed configuration (FRC) is a compact toroid with mostly poloidal magnetic field that is produced by the toroidal plasma current, and it has an extremely high-beta value [1, 2]. It can also be translated axially because it has a simply-connected geometry and does not require interlinked coils to produce the confining magnetic field. Because of these characteristics, The FRC has been expected to be a core plasma for advanced fuel (D-^{3}He and p-^{11}B) fusion reactors.

The C-2 series of large-size FRC devices at TAE Technologies, Inc., have succeeded in producing merged FRCs with large poloidal fluxes and long lifetimes *via* the collisional merging of two FRCs. It has been confirmed that FRC performance is improved by neutral-beam injection and edge biasing [3]. However, additional FRC heating techniques are limited because of the unique characteristics of FRCs, such as their extremely high beta and simply-connected geometries. It has therefore been proposed to use the excitation of low-frequency waves in an FRC as an additional heating technique. This technique was employed in the FIX (FRC Injection Experiment) device at Osaka University [4, 5]. The low-frequency wave was excited in the FRC by applying an oscillating magnetic field, and heating was experimentally verified.

To obtain central heating of an FRC, the excited wave must reach the core region. Figure 1 shows the propagation characteristics of the excited waves in the FAT-CM FRC, as determined from a CMA diagram based on the Rigid-Rotor (RR) profile model [6]. For Alfvén-wave heating, the energy is absorbed during mode conversion from a compressional to a shear Alfvén wave. Since the compressional Alfvén wave can be propagate vertically to the confinement magnetic field, we consider O and X waves on the diagram. Waves between 200 kHz and 100 GHz are reflected or resonant outside the separatrix of the FRC and cannot reach the FRC core. Thus, the frequencies of the waves must be lower than ∼200 kHz or higher than ∼100 GHz; these conditions correspond to the frequencies of the waves being lower than the ion cyclotron frequency and higher than the electron plasma frequency. We have

author's e-mail: asai.tomohiko@nihon-u.ac.jp

*) This article is based on the presentation at the 12th International Conference on Open Magnetic Systems for Plasma Confinement (OS2018).

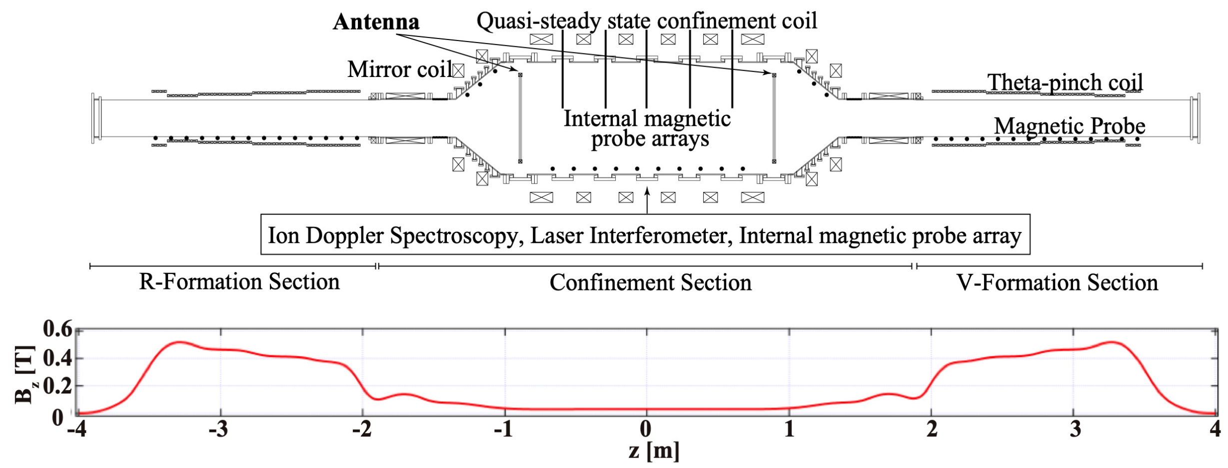

Fig. 2 Schematic drawing of the FAT-CM device (top) and a profile of the external guide magnetic field (bottom).

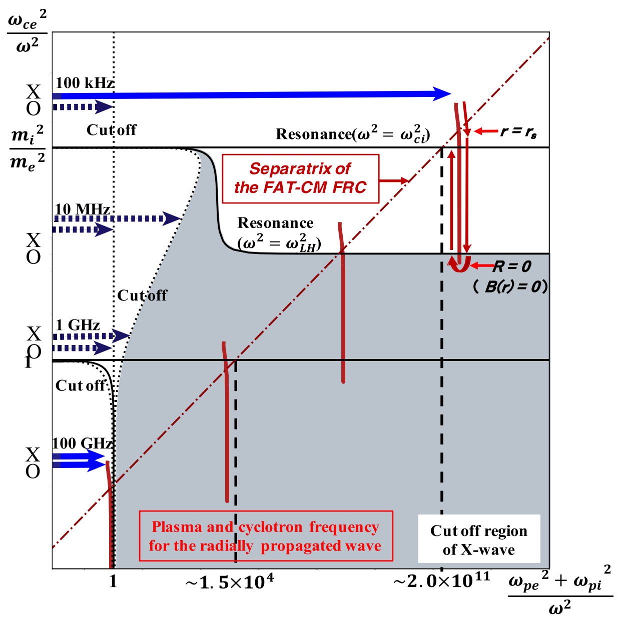

Fig. 1 CMA diagram for the FAT-CM device; both axes are logarithmic. Solid lines and dashed lines represent resonance and cutoff boundaries, respectively. The bold black lines represent the plasma and cyclotron frequencies in the radial direction for the RR profile [6]. The top of the figure is just outside the separatrix, and the bottom is the magnetic-field null. The dot-dash line represents the values at the separatrix.

therefore focused on the low-frequency band for exciting Alfvén waves in the present work.

At Nihon University, the FAT-CM device [7] has been developed to generate FRCs by collisional merging, producing target plasmas to be excited by low-frequency waves. We have also developed wave-excitation antennas and power supplies and have installed them in FAT-CM to excite waves in the FRCs contained in the confinement section of this device.

2. Experimental Apparatus

2.1 The FAT-CM device

The FAT-CM device consists of three sections: two formation sections and a central confinement section (Fig. 2). The confining magnetic field is approximately 0.08 T, with a mirror magnetic field of ~0.2 T; the mirror ratio is 2.5 - 3.5, and the distance between the mirrors is ~3.4 m.

Two FRC plasmas are formed simultaneously by field-reversed theta-pinches (FRTPs) in the two formation sections. Deuterium gas is puffed in from the end of each formation section. An initial FRC, with a radius of ~0.06 m and a length ~1.0 m, is formed in each formation section.

In the formation and confinement sections of the FAT-CM device, we have deployed various diagnostic instruments to measure the collisional merging and relaxation process of the FRCs. In the formation sections, 14 pickup coils and two flux loops are installed to define the excluded flux radius [8]. In the confinement section, an axial B_z magnetic-probe array consisting of 10 magnetic probes arranged at 0.15 m intervals is installed at $r \sim 0.35$ m, and three pickup coils are installed on both tapered end parts of the confinement section. At the midplane, an infrared (3.39 μm) He-Ne laser interferometer, an ion Doppler-spectroscopy system, and an internal magnetic-probe array [9] are installed. The ion Doppler-spectroscopy system measures the Doppler broadening of CIII (229.687 nm) or CIV (227.091 nm). In addition, five internal magnetic-probe arrays are installed at the axial positions $z = 0, \pm 0.3$, and ± 0.6 m to measure wave propagation near the separatrix of the merged FRC. These probe arrays consist of hand-wound pickup coils, three in the z-direction (B_z) and two in the θ-direction (B_t). The B_z coils are spaced 3 cm apart, and two of three B_z probes from the top of the array are placed together with the B_t probe. The probe positions are located at $r = 6$, 9, and 12 cm in device coordinates for a typical separatrix radius of 20 cm.

2.2 The wave-excitation antenna

To excite low-frequency waves in the merged FRC plasma, we have develooped loop antennas with discharge power supplies that use fast capacitor banks (2.4 µF). The antennas consist of two half-turn coils to decrease inductance and to change the frequency of the discharged current. The antennas have inner diameters of 600 mm, and they are encased in transparent quartz tube sheaths to maintain their one-turn loop shapes, as shown in Figs. 3 (a) and (b). The quartz tubes are installed through a Wilson seal in the confinement vessel. Although the antennas are placed at $z = 0.9$ and -0.9 m (Fig. 2), they can also be mounted in other axial positions. Also, the antennas are symmetric with respect to the geometrical axis and the midplane. In a previous study using the FIX device [4, 5], the single translated FRC made contact with the antenna during reflection at the end of the confinement section. By employing synmetric merging here, we expect the target FRC to be formed in the FAT-CM device without making contact with the antenna structure.

Figure 4 shows typical discharge waveforms for the antenna arrangement shown in Fig. 3. The frequency of the oscillating current can be varied by changing the coil inductance and the number of capacitor banks. In a discharge test performed in the metal confinement chamber, the frequencies of the oscillating currents were about 68 and 91 kHz for the antenna configurations shown in Figs. 3 (a) and 3 (b), respectively. For this antenna system, the upper limit to the frequency is approximately 100 kHz.

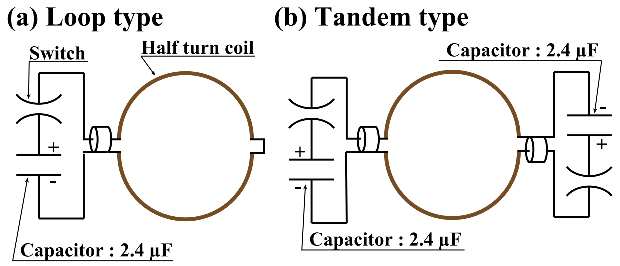

Fig. 3 Arrangements of the discharge circuits for the wave-excitation antenna.

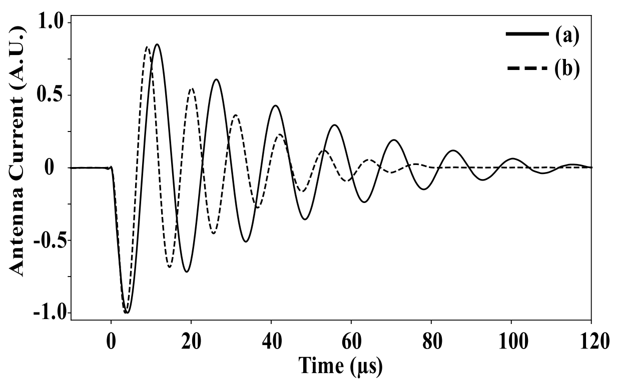

Fig. 4 Typical waveforms of the antenna current in the discharge test. The current values are normalized to show the difference in the frequencies produced by configurations 3 (a) and 3 (b).

3. Experimental Results

3.1 Formation of a target FRC plasma for low-frequency wave excitation

Figure 5 shows the time evolution of the axial profile of the excluded flux radius. The FRCs are translated simultaneously into the confinement section from the formation sections at ~30 µs after the main reversal. The translated FRCs collide around the midplane of the confinement section at ~50 µs. This forms a merged FRC structure, as confirmed by internal magnetic-field measurements. Figure 5 also shows that the plasmoids do not contact the antennas during the translation and collisional-merging processes.

The parameters of the merged FRC in the quiescent equilibrium phase are: excluded flux radius ~0.20 m, length ~1.8 m, volume ~7.6 × 10^{-2} m^3, average electron density ~1.0 × 10^{20} m^{-3}, total temperature ~100 eV, and stored energy ~800 J, respectively. The configuration lifetime—*i.e.*, (the *e*-folding time of the excluded-flux-radius signal—) is ~250 µs. The Alfvén velocity on the separatrix is ~120 km/s.

Figure 6 shows the radial variation of the ion cyclotron frequency in the merged FRC. We calculated the ion cy-

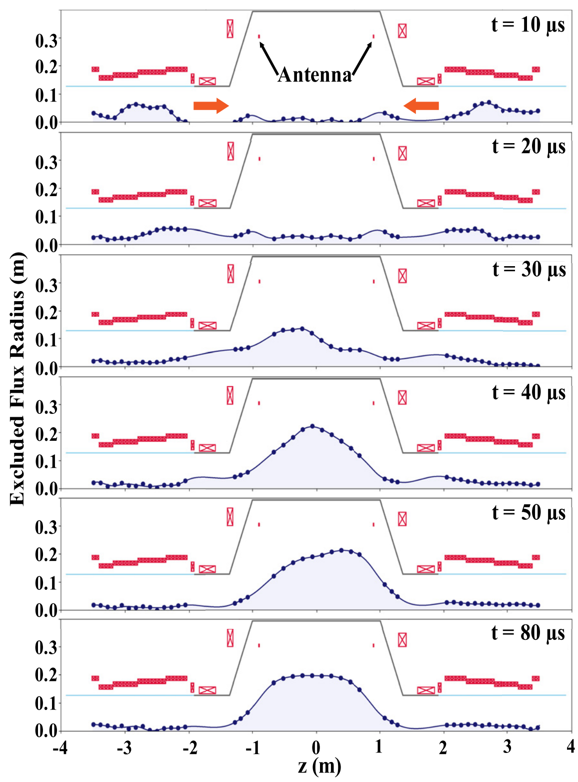

Fig. 5 Time evolution of the axial variation of the excluded-flux radius.

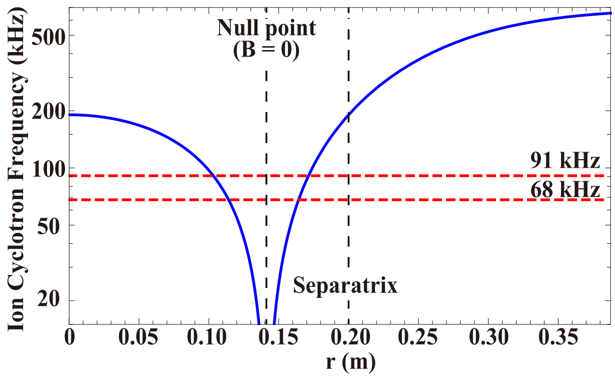

Fig. 6 Ion cyclotron frequency in the radial direction for the merged FRC.

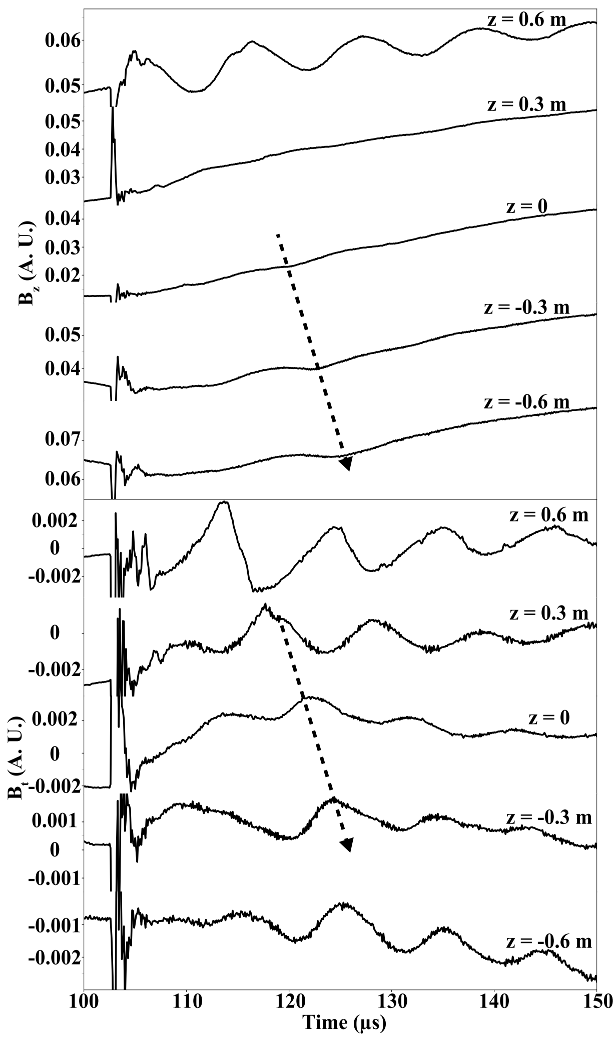

Fig. 7 The time evolution of the B_z (top) and B_t (bottom) signals from the internal magnetic-probe arrays (r = 9 cm).

clotron frequency for the RR profile model using the parameters of the merged FRC. From this figure, the ion cyclotron frequency on the separatrix of the merged FRC is ~190 kHz. The FRC parameters achieved thus satisfy the required condition shown in the CMA diagram (Fig. 1). In addition, the length of the merged FRC is longer than the wavelength of the excited wave (~1.3 m for f = 91 kHz). We calculated this wavelength as $L = V_A/f$, where V_A is the Alfvén velocity, and f is the frequency of the applied antenna current. Further, since the lifetime of the configuration is sufficiently long compared with a cycle of the antenna current (~11 μs or ~15 μs, respectively), the merged FRC has a long-enough configuration lifetime to sustain the oscillating magnetic field. Thus, the merged FRC is an appropriate target for the excitation of low-frequency waves.

3.2 Response of the target FRC plasma to low-frequency wave excitation

We therefore applied an oscillating magnetic field to the merged FRC. The experimental conditions were: antenna charging voltage = 15 kV, antenna current = 22 kA, stored energy of the fast capacitor banks = 1 kJ, frequency = 91 kHz, and e-folding time = 29 μs. In this experiment, we discharged only the V-formation-side antenna. Figure 7 shows the time evolution of the B_z and B_t signals from the internal magnetic-probe arrays; the radial position is near the null point of the merged FRC (r = 9 cm). The probe signals for both B_z and B_t oscillate during the antenna discharge. Also, we infer that the excited wave propagates in the axial direction, because the signals from the axially arranged probe arrays show phase differences, as indicated by the dotted arrows in Fig. 7. The propagation speed of ~60 km/s is comparable to the Alfvén velocity in the vicinity of the separatrix (~50 km/s). The input power to the antenna was ~28 MW in this case. For comparison, the loss rate of total stored energy is approximately 3 MW for the same experimental condition.

4. Summary

In the FAT-CM device, we have produced a target FRC plasma for low-frequency wave excitation; it has a lifetime longer than the e-folding time of the oscillating magnetic field and a length comparable to the wavelength of the excited wave. Since the frequency of the oscillating magnetic field is lower than the ion cyclotron frequency on the separatrix of the merged FRC, we expect the excited wave to be able to propagate into the separatrix of the FRC.

We observed excited-wave oscillations in the internal magnetic-field signals, and the oscillation period corresponds to the duration of the oscillatory current in the antennas. We conclude that an Alfvén wave was excited and propagated into the merged FRC with a propagation speed comparable to the predicted Alfvén velocity in the vicinity of the separatrix. We will report the details of these wave-excitation experiments elsewhere in the near future.

Acknowledgments

The authors would like to thank past and present members of our laboratory. This work was partially supported by JSPS KAKENHI Grant Number JP16K06939 and Grants-in-Aid of College of Science and Technology, Nihon University.

[1] M. Tuszewski, Nucl. Fusion **28**, 2033 (1988).
[2] L.C. Steinhauer, Phys. Plasmas **18**, 070501 (2011).
[3] M.W. Binderbauer *et al.*, Phys. Plasmas **22**, 056110 (2015).
[4] K. Yamanaka *et al.*, Phys. Plasmas **7**, 2755 (2000).
[5] S. Okada *et al.*, Nucl. Fusion **41**, 5 (2001).
[6] W.T. Armstrong *et al.*, Phys. Fluids **24**, 2068 (1981).
[7] T. Asai *et al.*, in 27th IAEA-FEC 2018, Gandhinagar, India (2018) EX/P7-20.
[8] M. Tuszewski *et al.*, Rev. Sci. Instrum. **54**, 1611 (1983).
[9] H. Gota *et al.*, Rev. Sci. Instrum. **89**, 10J114 (2018).